Available online at www.sciencedirect.com
SCIENCE DIRECT®
Acta Materialia 52 (2004) 5427–5433
Acta MATERIALIA
www.actamat-journals.com

Site preference and alloying effect of platinum group metals in γ'-Ni_3Al

C.Y. Geng [a,*], C.Y. Wang [a,b], T. Yu [a]

[a] Central Iron and Steel Research Institute, Beijing 100081, China
[b] Department of Physics, Tsinghua University, Beijing 100084, China

Received 19 April 2004; received in revised form 2 August 2004; accepted 8 August 2004

Abstract

Using supercell method, the alloying effect of platinum group metals (PGMs) on the lattice parameters of γ'-Ni_3Al and the site preference of these elements are systematically studied based on first-principle full-potential linearized augmented-plane-wave method. Due to the addition of PGMs, the lattice parameters of γ' is increased in the order: Mo < Rh < Ru < Ir < Pd < Os < Pt. The calculated site preference energies show that there are three site preference behaviors for PGMs additions in γ'. The calculations of cohesive energies show that Mo and Ru can stabilize the γ' phase, further in order to better explain the alloying effect of the two elements in the γ'-Ni_3Al, the impurity-induced charge density characteristics and the partial density of states are calculated for the systems containing Mo or Ru. The results show that the alloying effect of the two elements in the γ'-Ni_3Al is different.

Keywords: Site preference; Platinum group; Nickel aluminides; FLAPW; Electronic structure

1. Introduction

As a promising high-temperature structural material with remarkable mechanical properties, Ni-base superalloys have been developed for use in elevated temperatures applications. The key microstructure of such superalloys is the cubic $L1_2$ intermetallic compound Ni_3Al (the γ' precipitate) that is coherent with the face-centered Ni-rich solid solution (the γ matrix). The superalloys derive their outstanding high-temperature strength mostly from solid-solution hardeners in the γ matrix and ordered strengthening in the γ' precipitated phase that is an ordered (cubic $L1_2$) structure with nickel atoms at face centers and aluminum atoms at cube corners. A substitutional ternary addition in γ' phase may occupy exclusively the Al sites, the Ni sites, or appear on both types of sites. Clearly, knowledge about the preferential site substitution behavior of the alloying elements in the γ' phase is useful in elucidating the role of ternary additions for controlling the mechanical properties of Ni-base superalloys.

Several different theoretical approaches have been used to predict the site preference. The first attempt to understand the alloying behavior was made in 1959 with a phenomenological thermodynamic model [1], which suggested that the site substitution behavior of ternary additions to Ni_3Al was governed by the electronic structure of the ternary addition. Sixteen years later, Rawlings and Staton-Bevan [2] established the existence of a strong correlation between the site occupation of the ternary additions and the mechanical properties of the γ' phase. Following this pioneering work, the Miedema model by Ochiai et al. [3], the cluster variation method by Tso et al. [4], a pseudopotential orbital radii based structure maps by Raju et al. [5], and many electronic structure calculations [6–14] have been applied to study the site preference of many alloying elements in γ' phase.

* Corresponding author. Tel./fax: +86 10 6218 2756.
E-mail address: gengcuiyu122@sohu.com (C.Y. Geng).

1359-6454/$30.00
doi:10.1016/j.actamat.2004.08.007

In spite of considerable theoretical efforts, there still remain problems to be resolved. Because of the beneficial role of Ru in the fourth generation single crystal superalloy [15], much attention has recently been paid to platinum group metals (PGMs), such as Mo, Ru, Rh, Pd, Os, Ir, and Pt. Since PGMs usually have high melting points and high hot corrosion resistance, addition of PGMs is expected to enhance high temperature mechanical properties and hot corrosion resistance. Therefore we expect that a fairly high amount of PGMs can be alloyed in contrast to Re which assists the formation of a topologically close-packed (TCP) phase that resulting in deteriorating the creep properties. However, there are few reports investigating the alloying effect of PGMs addition in Ni-base alloys [16,17]. To the author's best knowledge, there is no direct experimental evidence for site preference of Ru, Rh and Os in Ni_3Al. Moreover, there are conflicts for the site preference of some PGMs in the theoretical calculations. So in an attempt to clarify the site substitution and to understand the alloying effect of PGMs in Ni_3Al, we performed a first-principle electronic structure calculation based on the FLAPW method [18], in the hope of providing a theoretical basis for understanding the experimental data, also, these results will provide a basis for further studying the role of PGMs additions in controlling the mechanical properties of Ni-base superalloys.

The paper is organized as follows. In Section 2, we briefly describe the supercell models and the first-principle FLAPW method used in our calculation. Section 3.1 presents the site preference of PGMs additions to γ'-Ni_3Al and makes a comparison with experimental data and other theoretical determinations. Section 3.2 presents the results of the changes in the electronic structure induced by Mo or Ru in γ'-Ni_3Al. Finally, a brief summary and statement of conclusions are presented in Section 4.

2. Method and computational model

All calculations reported in this paper are performed using the self-consistent full-potential linearized augmented-plane-wave method (FLAPW) based on the density functional theory [19]. The FLAPW method is renowned to be one of the most precise electronic structure and total energy method [20]. In the FLAPW method, no shape approximations are made to the charge densities, potentials, and matrix elements. The core states are treated fully relativistically and the valence states are treated semirelativistically (i.e., without spin–orbit coupling). The total and partial density of states (DOS) was obtained using a modified tetrahedron method of Blöchl et al. [21]. All our calculations have been performed with the generalized gradient approximation (GGA) [22].

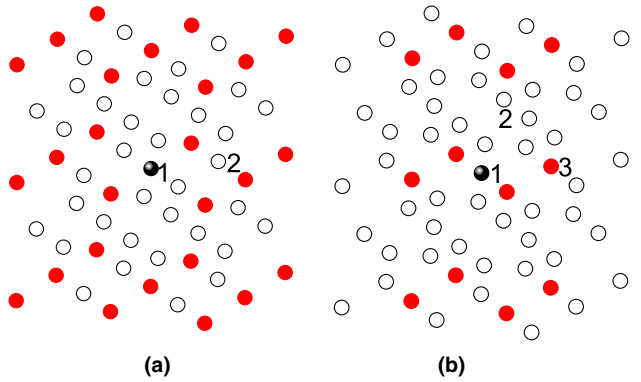

Fig. 1. (a) The 32-atom $Ni_{24}Al_7X$ supercell. X represents Al or PGMs atom. The central atom is labeled by the Arabic numeral 1, and the nearest neighbor (NN) Ni atoms are labeled by the numeral 2. (b) The 32-atom $Ni_{23}Al_8X$ supercell. X represents Ni or PGMs atom. The central atom is labeled by the Arabic numeral 1, the NN Ni atoms are labeled by the numeral 2, and the NN Al atoms are labeled by the numeral 3. The metallic, open and solid circles in (a) and (b) represent X, Ni, and Al atoms, respectively.

Two 32-atom supercells are employed in our calculations in which the center is either a Ni or Al, shown in Fig. 1. By doing the substitution, the PGMs atom X (such as Mo, Ru, Rh, Pd, Os, Ir, and Pt) is placed at the center of the supercells, occupying either a Ni or Al site. The supercells are constructed from 2^3 unit cells of Ni_3Al. Inequivalent atoms in the cell are denoted by numerical label, depending on their point-group symmetry. As Ni_3Al crystallizes in the cubic $L1_2$-type structure, in the present calculations, the total energy was minimized only with respect to the unit cell volume. In the calculation of site preference section, the atomic relaxation effect was neglected. Since the differences between the atomic radius of PGMs atoms and the host atoms are rather small. It is reasonable to expect that the relaxation would affect the site preference mildly. In order to check this idea, in the calculation of electronic structure section, the atomic relaxation around the Ru and Mo atoms is determined, which shows the maximum relaxation energy of only 0.0064 Ry. Therefore, it is reliable to neglect the atomic relaxation effect in the study of site preference in γ'-Ni_3Al. For simplicity, the same muffin-tin radii 2.3 a.u. was chosen for Al, Ni, and X atoms. The calculations have been performed on a $(8 \times 8 \times 8)$ k-points mesh in the Brillouin zone. The $R_{MT}K_{max}$ cutoff used is equal to 8 and the convergence criterion is 10^{-4} Ry. Our calculations are spin-restricted (without spin polarization).

3. Results and discussion

3.1. Site preference and alloying effect of PGMs additions in γ'-Ni_3Al

The total energy for X either at Ni or Al site should be known in order to judge the site preference of PGMs

atom X in γ′-Ni_3Al. The calculations of energy versus volume have been performed to optimize the sizes of the pure supercells and X contained supercells. The equilibrium lattice constant a, the minimum energy E_{tot} and the cohesive energy E_{coh} obtained by the FLAPW method for the pure supercells and the PGMs atom X contained supercells are summarized in Table 1. It can be seen from Table 1, for the pure supercells in which the center is either a Ni or Al, we obtain the lattice constants (a = 13.4858 a.u. (13.4869 a.u.)), which agree well with the experimental value [23] ($a = 6.7427 \times 2 =$ 13.4854 a.u.). Therefore, with this degree of precision we can determine the site preference of PGMs atom X in γ′-Ni_3Al. It is also clear seen that, in comparison with pure supercells, the lattice parameters of γ′-Ni_3Al are all increased by the addition of PGMs atom X. Moreover, as for the same PGMs atom X, the lattice parameter of $Ni_{23}Al_8X$ supercell is always larger than that of the corresponding $Ni_{24}Al_7X$ supercell. As is known, alloying elements affect γ′ mismatch with the matrix γ phase, and the degree of lattice mismatch between precipitate and matrix is related to the mechanical properties of Ni-base superalloys [25,26]. Therefore, the substitution behavior of a PGMs atom X in γ′-Ni_3Al should first be known in order to specify the lattice parameter change with additions of the element.

As seen in Table 1, we present the cohesive energy obtained by the FLAPW method for the Ni_3Al pure supercells and supercells with the substitution of an X atom. Table 2 lists the cohesive energy difference E_{dcoh} between the supercells in the presence of an X atom and the corresponding pure systems. It is clear seen that, in comparison with Ni_3Al pure supercells, only the cohesive energies of the systems containing Mo or Ru are lower. When a Mo (Ru) atom occupies an Al site, the cohesive energy decreases by as much as 0.2916 Ry (0.1542 Ry). When a Mo atom occupies a Ni site, the cohesive energy decreases by 0.0874 Ry; however, for a Ru atom, it decreases by 0.0787 Ry. These results imply that both Mo and Ru can stabilize the Ni_3Al phase, and that both have the possibility of occupying either an Al site or a Ni site.

Knowledge of the site preference energy is needed to describe the site substitution behavior of an X atom in the Ni_3Al phase. The energetics of the preferential bonding of X in γ′-Ni_3Al can be studied by the site preference energy, which is defined as the energy difference between two formation energies:

$$E_{site} = \Delta E_1 - \Delta E_2, \tag{1}$$

where ΔE_1, ΔE_2 are the formation energies of $Ni_{24}Al_7X$ and $Ni_{23}Al_8X$, respectively. Following Wolf et al. [27], the usual definition of formation energies ΔE_i is the total energy difference between compound and constituent elements in the solid state.

$$\Delta E_1 = E_{Ni_{24}Al_7X} - 24E_{Ni} - 7E_{Al} - E_X, \tag{2}$$

$$\Delta E_2 = E_{Ni_{23}Al_8X} - 23E_{Ni} - 8E_{Al} - E_X, \tag{3}$$

where E_{Ni}, E_{Al}, and E_X are the total energies of pure Ni, Al, and X, respectively. So we can deduce the form of E_{site} from the above two formation energies:

$$\begin{aligned} E_{site} &= \Delta E_1 - \Delta E_2 \\ &= E_{Ni_{24}Al_7X} - E_{Ni_{23}Al_8X} - E_{Ni} + E_{Al}. \end{aligned} \tag{4}$$

If $E_{site} < 0$, the substitution for Al is energetically more favorable, and if $E_{site} > 0$, X is rather on the Ni site. The total energy for pure bulk metal (per atom) is used to provide the reference energy for the constituent species. In our case, these are the total energies of fcc Ni and fcc Al. These have been calculated using the same FLAPW method and their values are

$$E_{Ni} = -3041.6547 \text{ Ry}, \tag{5}$$

$$E_{Al} = -485.6441 \text{ Ry}. \tag{6}$$

The calculated values of E_{site} are also presented in Table 2. From the values of E_{site}, we can determine the preference of each PGMs atom X in γ′-Ni_3Al (Table 3).

Table 2
The cohesive energy difference E_{dcoh} (in Ry) and the site preference energy E_{site} (in Ry) of PGMs additions in γ′-Ni_3Al

X	$E_{dcoh}^{Ni_{24}Al_7X}$	$E_{dcoh}^{Ni_{23}Al_8X}$	E_{site}
Mo	0.2916	0.0874	−0.0603
Ru	0.1542	0.0787	0.0729
Rh	−0.0466	−0.0572	0.1382
Pd	−0.1761	−0.1638	0.1609
Os	−0.1727	−0.2896	0.0291
Ir	−0.3213	−0.3602	0.1098
Pt	−0.5784	−0.5740	0.1517

Table 1
Equilibrium lattice constant a (in a.u.), total energy E_{tot} (in Ry), and the corresponding cohesive energy E_{coh} (in Ry) of $Ni_{24}Al_7X$ ($Ni_{23}Al_8X$) supercell, X stands for Al (Ni) or PGMs atom

X	$a^{Ni_{24}Al_7X}$	$E_{tot}^{Ni_{24}Al_7X}$	$E_{coh}^{Ni_{24}Al_7X}$	$a^{Ni_{23}Al_8X}$	$E_{tot}^{Ni_{23}Al_8X}$	$E_{coh}^{Ni_{23}Al_8X}$
Al(Ni)	13.4869	−76885.9829	−13.0413	13.4858	−76885.9828	−13.0412
Mo	13.5240	−84499.4522	−13.3329	13.5895	−81943.3883	−13.1286
Ru	13.5117	−85463.8946	−13.1955	13.5491	−82907.9595	−13.1199
Rh	13.5170	−85970.7044	−12.9947	13.5479	−83414.8343	−12.9841
Pd	13.5358	−86494.2409	−12.8653	13.5583	−83938.3935	−12.8774
Os	13.5080	−110964.1362	−12.8686	13.5632	−108408.1596	−12.7516
Ir	13.5204	−112116.4514	−12.7200	13.5581	−109560.5528	−12.6810
Pt	13.5454	−113293.6110	−12.4629	13.5737	−110737.7558	−12.4672

Table 3
The calculated site preference behavior and comparison with those reported in the literature

X	This work	Theory	Experiment
Mo	*A*	*A* Refs. [5,12,13], *a* Ref. [11]	*c* Ref. [24]
Ru	*N*	*N* Refs. [5,13], *a* Ref. [12]	
Rh	*N*	*N* Refs. [5,13], *n* Ref. [12]	
Pd	*N*	*N* Refs. [5,11,13], *n* Ref. [12]	*N* Ref. [28]
Os	*n*	*N* Ref. [13], *n* Ref. [5], *A* Ref. [12]	
Ir	*N*	*N* Ref. [13], *n* Ref. [5], *a* Ref. [12]	*A* Ref. [16]
Pt	*N*	*N* Refs. [5,13], *n* Ref. [12]	*N* Ref. [28]

An *A*(*N*) means a strong Al (Ni) site preference, and an *a*(*n*) indicates a weak site preference for the Al (Ni). Cases that it is known only that the site preference is neither *A* nor *N* type have been given with the letter *c*. "Theory" refers to theoretical determinations reported in the literature, and "experiment" refers to a variety of experimental determinations.

It can be seen from Table 3 there are three fundamental site preference behaviors for PGMs additions in γ'-Ni_3Al: Mo prefers the Al site; Os has a weak site preference for the Ni site; while the other PGMs atoms such as Ru, Rh, Pd, Ir, and Pt prefer the Ni site, and this preference increases in the order: Ru < Ir < Rh < Pt < Pd. Our results for the Pd and Pt site preference in γ'-Ni_3Al are the same as those of Raju [5], Sluiter [11], and Chen [13], and are also consistent with the experiment result [28]. While the calculation of Ruban and Skriver [12] shows that Pd and Pt only have a weak site preference for the Ni site. As for the Ir case, there is one experiment in which points out Ir occupying Al site [16]. Besides Ruban' calculation [12], all the other theoretic research including this work indicates that Ir prefers to Ni sites. One reason for discrepancies between theoretic and experiment result may be seen that, in fact theoretic study are within one phase region (γ'-Ni_3Al), and our calculations are based on the model of a perfectly ordered crystal. For the site preference of Mo, Ru, Rh, and Os, no experimental result is available. According to our results, we predict Mo prefers to Al site, Os has a weak site preference for the Ni, while Ru and Rh occupy Ni sites in γ'-Ni_3Al. This coincides with most of the theoretical results, as shown in Table 3. In addition, after the site preference is reliably determined, we can further to study of the alloying effect. From Tables 1 and 3, we can easily see the lattice parameter due to the addition of PGMs atom is determined to increase in the following order: Mo < Rh < Ru < Ir < Pd < Os < Pt. The above results provide a basis for further studying the effects of PGMs atom in improving the mechanical properties of Ni-base superalloys.

3.2. Electronic structure changes induced by Mo or Ru in γ'-Ni_3Al

In this section we are to study the electronic mechanism inclined by the alloying effect of Mo (Ru) when occupying an Al (Ni) site in γ'-Ni_3Al. In the calculation, relaxation around the X atom is determined via FLAPW relaxation calculation. For a given supercell volume, only the twelve nearest neighbors and the six next nearest neighbors of the Mo (Ru) are considered to relax, and preserve the symmetry during relaxation. The relaxation results show that when Mo occupies an Al site, the nearest neighbor (NN) Ni2 atoms and the next nearest neighbor (NNN) Al3 atoms are almost completely undisturbed. While noticeable lattice distortions of NN atoms appear when Ru substitutes for Ni site. The NN Ni2 atoms sites around Ru atom expand by 1.1% of the calculated lattice constant, and the NN Al3 atomic sites around Ru atom expand by 1.6% of the calculated lattice constant. The calculated relaxation energy E_R of Ru is listed in Table 4. We use the following definition for the relaxation energy:

$$E_R = E_r(a_r) - E_u(a_u). \tag{7}$$

With a_u and a_r being the lattice constants that give the minimum energy for the unrelaxed (E_u) and relaxed (E_r) configurations, respectively. The result given in Table 4 shows the relaxation energy of only 0.0064 Ry. Since the relaxation energy is relatively small, it is reliable to neglect the relaxation around the X atom in the study of site preference in γ'-Ni_3Al. That is the reason why previous first-principle investigations [6–12] on the site substitution of Ni_3Al do not consider the atomic relaxation effect. While in order to undertake a more precise study of the electronic mechanism underlying the alloying effect, we think it is necessary to take into account this effect.

To understand the effect of alloying atoms on the bonding properties of Ni_3Al, we consider the redistribution of charge induced by the alloying atoms when substituted for Ni (or Al). The charge density differences are plotted in Figs. 2 and 3. For the $Ni_{24}Al_7Mo$ system, the charge density can be defined as:

$$\Delta\rho = \rho(Ni_{24}Al_7Mo) - \rho_{free}(Ni_{24}Al_7Mo) - \rho(Ni_{24}Al_8) + \rho_{free}(Ni_{24}Al_8). \tag{8}$$

Here $\rho(Ni_{24}Al_8)$ is the charge density of the supercell with Al at the center. For the $Ni_{23}Al_8Ru$ system, we can write out the similar definition:

$$\Delta\rho = \rho(Ni_{23}Al_8Ru) - \rho_{free}(Ni_{23}Al_8Ru) - \rho(Ni_{24}Al_8) + \rho_{free}(Ni_{24}Al_8). \tag{9}$$

Table 4
Equilibrium lattice constant a_r for fully relaxed $Ni_{23}Al_8Ru$ supercell, its total energy E_r, and the corresponding relaxation energy E_R (relative to the unrelaxed $Ni_{23}Al_8Ru$ supercell)

a_r (a.u.)	E_r (Ry)	E_R (Ry)
13.5433	−82907.9659	0.0064

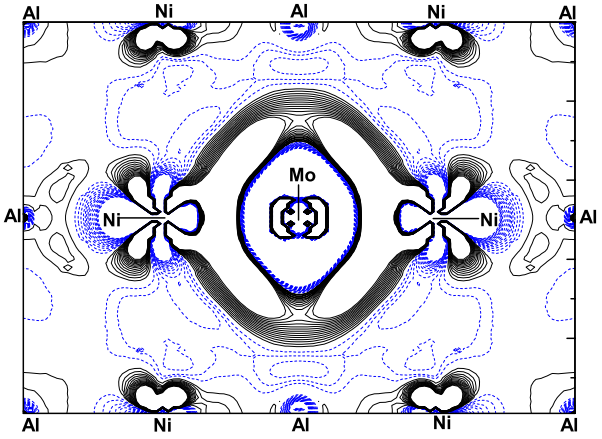

Fig. 2. The electron density difference on the (1 1 0) plane between the $Ni_{24}Al_7Mo$ system and the Ni_3Al system with Al at the center. The contour spacing is 0.0001 e a.u.$^{-3}$. Solid lines and dashed lines correspond to the increased and the decreased charge density, respectively.

Here $\rho(Ni_{24}Al_8)$ is the charge density of the supercell with Ni at the center. From Fig. 2, we can see that charge correlation regions due to the electron accumulation appear around the Mo atom and the NN Ni2 atoms. This means the bonding for Mo and its NN Ni2 atoms is stronger than that for Al and its NN Ni2 atoms when Mo substituted for Al, which reflecting enhanced interactions between Mo and NN Ni2 atoms in $Ni_{24}Al_7Mo$ system. Thus there forms the relative strong bonding that has covalence-like character between Mo and NN Ni2. In Fig. 3, we have given the charge density plotted in different planes in order to show the bonding for Ru and its NN Ni2 and NN Al3 atoms. It can be seen from Fig. 3(a) and (b), the charge density between the Ru and the NN atoms, which include both Ni and Al atoms, are decreased relative to that in the pure Ni_3Al system. On the other hand, the charge density between the NN Ni2 atoms themselves as well as between the NN Ni2 atoms and its nearest neighbor Ni atoms is apparently increased which can be seen from Fig. 3(b). This is different from Mo effect. These results provide concrete information giving insight into the alloying effects for Mo and Ru atoms.

In order to analyze the interactions between the alloying element and its NN host atoms further, we calculated the partial density of states (PDOS). PDOS for the center X, the NN Ni2 and NN Al3 atoms of the four different systems are shown in Figs. 4(a)–(d). The density of states in the Ni_3Al systems agrees well with the existing calculation [6]. Besides the strong Ni d–d bonding, it can clearly be seen from Fig. 4(a) and (c) that a sharp bonding peak and antibonding peak is located near −3 and 1.2 eV, which shown there is hybridization between Ni d and Al p states. Another feature of the electronic structure for Ni_3Al systems is a valley located at about 0.5 eV above the Fermi energy, which separated the p–d bonding and antibonding states. For the $Ni_{24}Al_7Mo$ system, we can see that from Fig. 4(a) and (b) the main peaks of the s and p states of Mo are located in the higher energy region relative to that of Al, thus there is much bigger overlap between Mo-s and Ni2-d and Mo-p and Ni2-d states over the whole energy spectrum. As a result, the hybridization between Mo and its NN Ni2 atoms is stronger than that for Al and the corresponding atoms. We can also see that, as the primary contribution to the bonding between the Mo atom and the NN Ni2 atoms, Mo-d state hybridize strongly with the s, p, and d states of NN Ni2 atoms; In contrast, the Al atom has no d state, so this also makes the interaction between Mo and its NN Ni2 atoms

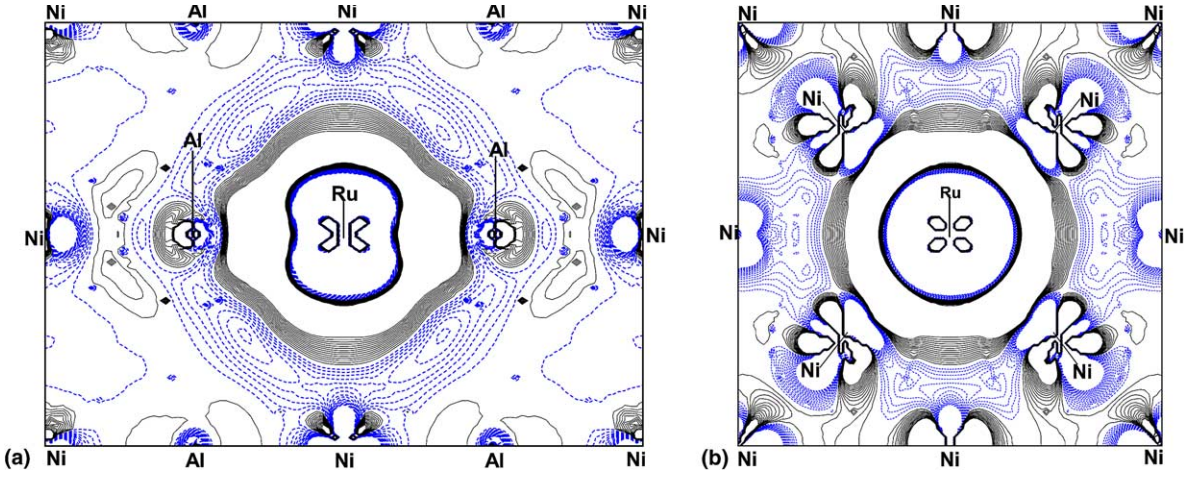

Fig. 3. The electron density difference on the (a) (1 1 0) plane, and (b) (2 0 0) plane between the $Ni_{23}Al_8Ru$ system and the Ni_3Al system with Ni at the center. The contour spacing is 0.0001 e a.u.$^{-3}$. Solid lines and dashed lines correspond to the increased and the decreased charge density, respectively.

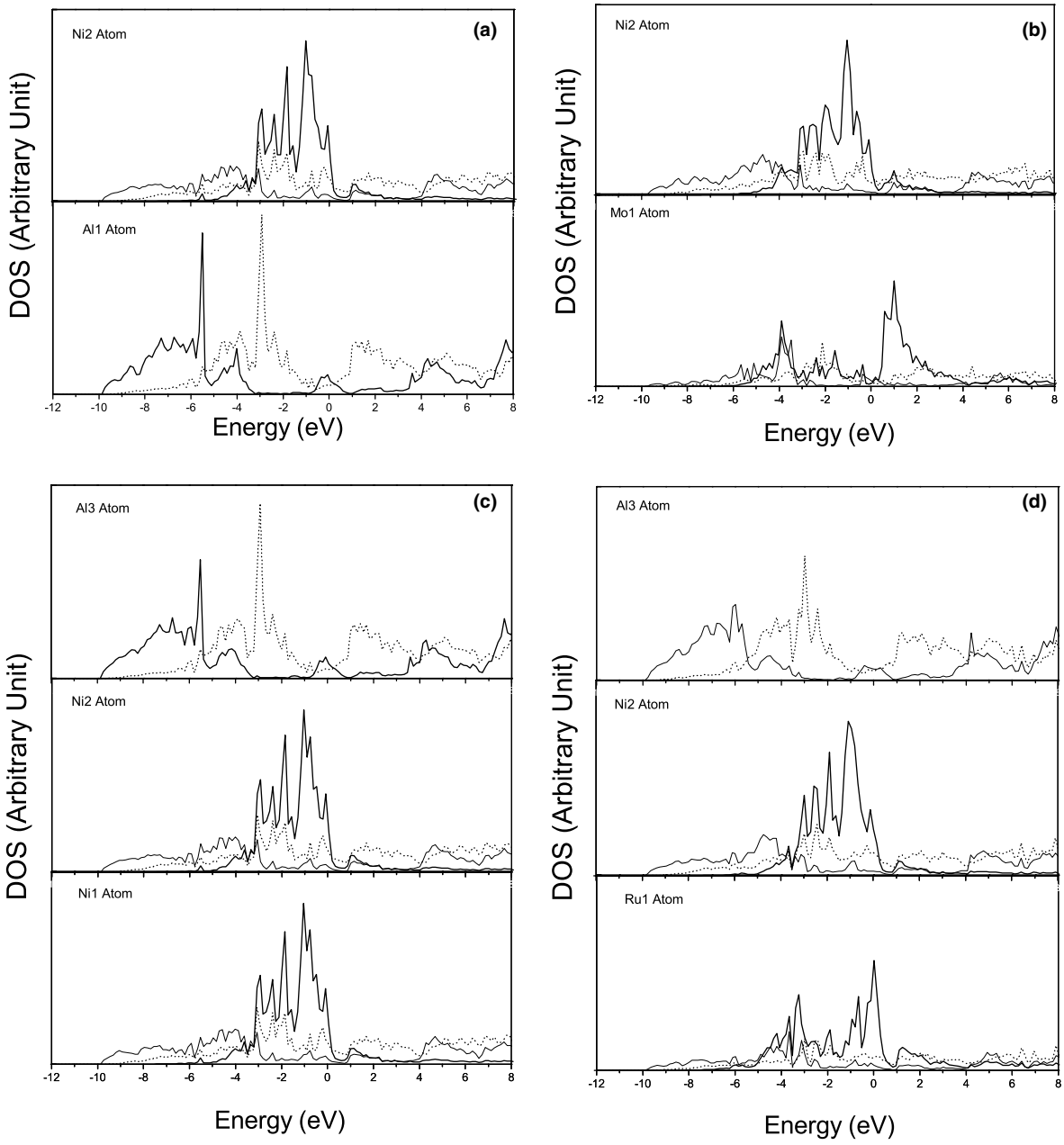

Fig. 4. The atomic partial density of states in (a) the Ni_3Al system with Al at the center, (b) the $Ni_{24}Al_7Mo$ system, (c) the Ni_3Al system with Ni at the center, and (d) the Ni_{23} Al_8Ru system. The thick solid lines, thin solid lines and dashed lines denote d, s, and p partial density of states, respectively. The Fermi level is shifted to zero. The Arabic numbers in Al1, Ni2, etc., correspond to those in Fig. 1.

very strong. For the $Ni_{23}Al_8Ru$ system, from Fig. 4(c) and (d) we can see that the PDOS curves of the Ni2-4s, 4p and Al3-3s, 3p states are considerably changed in the whole energy region. While the PDOS curve of the Ni2-3d state shows some small changes around -3.8 and -0.8 eV. In Fig. 4(d), some clean and isolated PDOS peaks of Ru appear at both sides of the Fermi level, resulting from the very weak interactions between the states of the Ru atom and those of the host Ni2 atoms. The above results are consistent with the analysis on charge density.

4. Conclusions

We have determined the lattice parameters and site preference of PGMs additions in γ'-Ni_3Al by the first-principle total energy calculations using supercell models. The results for the site preference energies suggest Mo prefers the Al site, and Os has a weak site preference for the Ni site, while the other PGMs atoms such as Ru, Rh, Pd, Ir and Pt exhibit a Ni preference. The lattice parameter due to the addition of PGMs atom is determined to increase in the following order:

Mo < Rh < Ru < Ir < Pd < Os < Pt. The calculated results clearly show that only Mo and Ru have a tendency to stabilize the Ni_3Al phase, and the alloying effect of the two elements in the γ'-Ni_3Al is different. The substitution of Mo exhibits strong interactions with the NN Ni2 host atoms, while the effect of Ru enhances the interaction between NN Ni2 atoms themselves as well as between the NN Ni2 atoms and its nearest neighbor Ni atoms.

Acknowledgements

We thank Professors P. Blaha et al. for giving us their first-principles program WIEN2k. We are also grateful to Professor J.T. Wang for beneficial discussions. This work is supported by "973 Project" from the Ministry of Science and Technology of China (Grant No. TG2000067102) and the National Natural Science Foundation of China (Grant Nos. 90306016 and 901041044).

References

[1] Guard RW, Westbrook JH. Trans Metall Soc AIME 1959;215:810.
[2] Rawlings RD, Staton-Bevan AE. J Mater Sci 1975;10:505.
[3] Ochiai S, Oya Y, Suzuki T. Acta Metall 1984;32:289.
[4] Tso NC, Sanchez JM. Mater Sci Eng A 1989;108:159.
[5] Raju S, Mohandas E, Raghunathan VS. Scripta Mater 1996;34:1785.
[6] Xu JH, Oguchi T, Freeman AJ. Phys Rev B 1987;36:4186.
[7] Min BI, Freeman AJ, Jansen HJF. Phys Rev B 1988;37:6757.
[8] Xu JH, Min BI, Freeman AJ, Oguchi T. Phys Rev B 1990;41:5010.
[9] Cao JC, Liu FS, Wang CY. J Phys F 1988;18:1839.
[10] Yang JL, Xiao CY, Xia SD, Wang KL. J Phys: Condens Matter 1993;5:6653.
[11] Marcel H, Sluiter F, Kawazoe Y. Phys Rev B 1995;51:4062.
[12] Ruban AV, Skriver HL. Phys Rev B 1997;55:856.
[13] Shen J, Wang Y, Chen NX, Wu Y. Progr Nat Sci 2000;10:457.
[14] Wang SY, Wang CY, Sun JH, Duan WH, Zhao DL. Phys Rev B 2001;65:035101.
[15] Argence D, Vernault C, Desvallees Y, Fournier D. In: Pollock TM, Kissinger RD, Bowman RR, Green KA, Mclean M, et al, editors. Superalloys 2000. TMS; 2000. p. 829.
[16] Murakami H, Koizumi Y, Yokokawa T, Yamabe-Mitarai Y, Yamagata T, Harada H. Mater Sci Eng A 1998;250:109.
[17] Murakami H, Honma T, Koizumi Y, Harada H. In: Pollock TM, Kissinger RD, Bowman RR, Green KA, Mclean M, et al, editors. Superalloys 2000. TMS; 2000. p. 747.
[18] Blaha P, Schwarz K, Madsen G, Kvasnicka D, Luitz J. Computer Code WIEN2k, Vienna University of Technology, Vienna; 2003; Improved and updated version of original code published by Blaha P, Schwarz K, Sorantin P, Trickey SB. Comput Phys Commun 1990;59:399.
[19] Hohenberg P, Kohn W. Phys Rev 1964;136:B864;
Kohn W, Sham LJ. Phys Rev 1965;140:A1133.
[20] Singh DJ. Planewaves, pseudopotentials and the LAPW method. Boston (MA): Kluwer Academic; 1994.
[21] Blöchl P, Jepsen O, Andersen OK. Phys Rev B 1994;49:16223.
[22] Perdew JP, Burke K, Ernzerhof M. Phys Rev Lett 1996;77:3865.
[23] Hackenbracht D, Kubler J. J Phys F 1983;13:L179.
[24] Loomis WT, Freeman JW, Sponseller DL. Metall Trans 1972;3:989.
[25] Mishima Y, Ochiai S, Suzuki T. Acta Metall 1985;33:1161.
[26] Lahrman DF, Field RD, Darolia R, Fraser HL. Acta Metall 1988;36:1309.
[27] Wolf W, Podloucky R, Rogl P, Erschbaumer H. Intermetallics 1996;4:201.
[28] Chiba A, Shindo D, Hanada S. Acta Metall 1991;39:13.